ELSEVIER

Surface tailoring control in micelle templated silica

Alireza Badiei [a,*], Laurent Bonneviot [b], Nicolas Crowther [b], Ghodsi Mohammadi Ziarani [c]

[a] *Department of Inorganic Chemistry, School of Chemistry, University Callege of Science, University of Tehran, P.O. Box 14155-6455 Tehran, Iran*
[b] *Laboratoire de Chimie, Ecole Normale Supérieure de Lyon, 46 allée d'Italie, F-69364 Lyon Cedex 7, France*
[c] *Department of Chemistry, Faculty of Science, Alzahra University, Iran*

Abstract

Surface tailoring control was studied using new concept surface-protector (SP) group that can covered a part of surface. In micelle templated silica, cationic surfactant had the role of SP group. Various methods of silylation on the surface coverage was done on the hexagonal micelle templated silicas and the samples was characterized using BET surface measurement, pore size distribution, FT-IR and ^{13}C and ^{29}Si MAS NMR. Direct silylation of micelle templated silica still containing the templating surfactant can lead to total or partial silylation of the internal (and external) surface depending on the silylation agent. A mixture of chlorotrimethylsilane in hexamethyldisiloxane leads to full coverage by trimethylsilyl groups and to a very hydrophobic surface. Using hexamethyldisilazane, the silylation drops down to 45–65% and displaces only partially the templating $CTMA^+$ surfactant. The displacement of the remaining surfactant molecules leaves behind hydrophilic nests of the size of the ammonium heads (~ 0.7 nm^2). Cation exchange can be performed on these nests at pH to 10 without structure collapse.
© 2006 Elsevier B.V. All rights reserved.

1. Introduction

The large pore of micelle templated silica (MTS) in comparison to that of zeolites provides novel opportunities in the field of molecular sieves not only for the scope of treating bulkier molecules but also for the variety of chemical modifications of their internal surface [1–5]. Taking advantages of such a versatility, researchers have tried to tailor tune their acid–base, their hydrophobicity and their catalytic properties envisioning many different applications in fields as different as adsorbents, separation and acid catalysis [6]. In this context, the stability of micelle templated silica is an important consideration. Originally, their hydrothermal stability was poor according to the loss of their mesoporous structure in acid or alkaline solution [7–9]. Several methods have been proposed to increase the stability of mesoporous materials, including synthesis

of materials with thicker pore walls [10–12], silylation [13–18], stabilization by tetralkylammonium [19], and salt effect [20,21]. New avenues are explored recently, where templated mesostructured materials have been designed with pore walls with an organic core and an inorganic shell using $(EtO)_3$ Si–R–Si$(OEt)_3$ (R = ethane, benzene and thiophene) type of precursors [22,23]. However, the organic functions are located inside the walls where again accessibility restriction is expected.

A more specific approach consists in fixing the organic functions at the surface of the wall by either covalently grafting various organic species into the channels [24–26] or incorporating functionalities directly during the preparation [15,27–30]. For instance, trimethylsilylation, which also increases the mechanical properties of the materials, allows producing highly hydrophobic materials [31]. In addition, it allows to increase the catalytic performance of Ti modified MTS in selective oxidation of alkenes into epoxides using H_2O_2 as oxidant agent [32]. The alkylsilylation on the as-synthesized form of the MTS may be

---

* Corresponding author. Tel.: +98 21 61112614; fax: +98 21 66405141.
  E-mail address: abadiei@khayam.ut.ac.ir (A. Badiei).

restricted to the external surface by using a silylating agent with a long alkyl chain [16]. Nonetheless, the templating surfactant filling pores is displaced using short alkyl chain silylation agent leading to alkylsilylation of the internal surface as reported for FSM-16 and lately for MCM-41 type of materials [18]. It has been also proposed to modify the window diameter opening by alkoxysilylation using TEOS and acetic acid directly on the as-synthesized form [33]. The strategy adopted in those last studies consists in taking advantage of the full occupancy of the internal volume by the templating surfactant. The surfactant displacement, where is the key point of these strategy is far from being fully understood.

For the sake of further surface tailoring control, we introduce *surface-protector* (*SP*) groups that can cover a part of surface. The SP groups prevent to surface tailoring by silylating agents. Thus the uncovered surface will be silylated, and then the SP group will be removed. These steps are schematically presented in Fig. 1. It is anticipated that surface tailoring depends on the number of SP group and covered surface by SP group. In as-synthesized MTS, cationic surfactants are electrostatically bonded to silanolate groups. Thus, it can act as a SP group. In this work, three different methods leading to various controlled silylation of the as-synthesized formed from of MTS are proposed. We shall demonstrate using XRD, N_2 adsorption–desorption isotherm, FT-IR, ^{13}C and ^{29}Si MAS-NMR techniques that controlled silylation may yield hydrophilic islands of very small size within the channel of these materials.

2. Experimental

2.1. Preparation of hexagonal MTS

Pure hexagonal MTS silica, is prepared from a gel of molar composition: $1.00SiO_2$, $0.86Na_2O$, $0.44(TMA)_2O$,
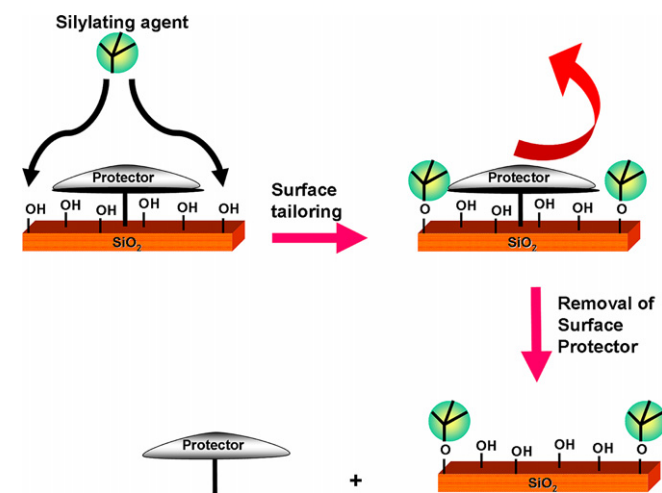

Fig. 1. The surface-protector (SP) cover a part of surface. These prevent to surface tailoring by silylating agents. Then, the uncovered surface is silylated and finally the SP groups are departed.

$0.30CTMABr$, $63.3H_2O$ (TMA = tetramethylammonium) [34]. Clear cetyltrimethylammonium bromide (CTMABr) solution is slowly added to a clear gel containing fumed silica (Cab-O-Sil), sodium silicate (Aldrich), and TMA-silicate (Sachem) with vigorous stirring at room temperature. The resulting gel is transferred into a Teflon-lined autoclave (1 L autoclave for about 60 g of silica) and maintained for 24 h at 130 °C. The resulting powder is filtered, washed with distilled water and dried in air. To improve the long range order of the as-synthesized material, the resulting solid is treated in 600 ml of water per 60 g of solid into a Teflon-lined autoclave for 24 h at 130 °C [35]. Then, this powder is filtered, washed with distilled water, and dried in air.

2.2. Trimethylsilylation of the MTS surface

All three silylation methods described below were performed directly on the as-synthesized MTS material dried at 100 °C. In method A, the solid (1.0 g) is treated overnight under reflux at 100 °C in 20 ml of a 1:1 mixture of chlorotrimethylsilane (CTMS) and hexamethyldisiloxane (HMDSO) [2,36,37]. In method B, the refluxing mixture is replaced by a solution of hexamethyldisilazane HMDSA (10 ml) and the solid (1.0 g) in toluene (40 ml) and allowed to react for 2 h at 110 °C [38]. In method C, the solid (1.2 g) is placed into a fluidized bed under a gas flow (15 cm³/min) of nitrogen saturated at 130 °C with HMDSA (5 ml was consumed). The silylated products are washed with ethanol and dried in air.

The chemical analysis of the solids and the SiO^- titration using HCl are performed as described earlier [39]. Typically, 250 mg of sample are added to a mixture of 100 ml of ethanol and 10 ml of 0.1 N HCl and stirred for 2 h. In this condition, the surfactant, which is removed from the solid, is filtered and washed with ethanol to obtain the so-called acid washed material. The excess of HCl is titrated with 0.1 N NaOH. The silylated materials are all tested for their ion exchange capacity after removal of the template using acid washing as described above. A chloride salt of the $[Co(en)_2Cl_2]^+$ complex is cation exchanged at room temperature for 1 h [40,41]. Typically, for 200 mg of silylated MTS and acid washed, 3 ml of concentrated ammonia (30%) is added to a 50 ml solution of cobalt complex (2.8×10^{-3} M) in a 73:27 water:ethanol mixture. The pH is approximately 10 at the end of the exchange treatment (note that the solid is too hydrophobic to adsorb pure water). Note that the conditions are slightly different from those previously reported, where the as-synthesized form was treated by a neutral solution of cobalt complexes [40,41].

2.3. Characterization

The XRD powder patterns of the samples were obtained using a Siemens D5000 diffractometer with the Cu Kα radiation ($\lambda = 1.54184$ Å). FT-IR measurements were

performed using a Bomen spectrometer in transmission mode on pellets (70 mg self supported wafer containing 1% of the sample in KBr). The latter were prepared by using a pressure of 5 ton/square inch. The fully silylated silicas which did not give stable pellet, were placed between two KBr windows.

Nitrogen adsorption–desorption profiles were obtained using an Omnisorp-100 apparatus. Adsorption isotherms were measured at −196 °C over the interval of relative pressures p/p_0 10^{-6} to 0.995. Before each analysis the samples were acid washed and outgassed for 2 h at 300 °C under vacuum. Such temperature did not remove the trimethylsilyl function from the surface according to FT-IR and chemical analysis.

^{13}C and ^{29}Si NMR measurements were carried out using a Bruker ASX 300 spectrometer at 75.4 MHz and 59.6 MHz, respectively. The samples were placed in a 7 mm zirconia rotor which was spun at a frequency of 5 kHz at magic angle. The measurements were performed at room temperature. The total number of scans for carbon and silicon were 800 and 1300, respectively. The repetition time was set at 10 s and 30 s for ^{13}C and ^{29}Si respectively to insure full longitudinal spin relaxation and to allow quantitative measurements. Cross polarization was not performed for the same reasons [42]. Chemical shift was referenced to tetramethylsilane.

3. Results

The XRD patterns of all the samples including acid washed silylated and ion exchanged samples exhibit four peaks in the 2θ range 1–6°, the spacing and intensity of which are consistent with the *P6m* space group of an hexagonal MTS of the MCM-41 type of structure (Fig. 2). The intensity of the XRD peaks increases dramatically after removal of the surfactant by acid washing, that can be explained by a higher contrast between walls and channels when the surfactant is removed. Oppositely, silylated and cobalt exchanged materials exhibit smaller XRD peaks, because the channels are partially occupied by the trimethylsilyl group and eventually the cobalt ions. However, the much higher decrease of intensity for the samples treated according to method A may indicate a loss of structure. The XRD peak positions do not change after partial silylation using HMDSA. By contrast, there is a shift of the peaks towards low diffraction angles when the silylating agent is CTMS (method A). Besides, the samples obtained from the latter method do not ion exchange cobalt and remain white. By contrast, for the other samples there is a color change from green to pink typical of a trans to cis isomerization of the octahedral dichloro bisethylendiammine cobalt (III) complex. This isomerization occurs during adsorption into the channels of the material. The UV–visible spectra are similar to those reported earlier on the adsorption of the same complex on amorphous silica and on non-silylated MTS [40,41]. In both case, the pink coloration can be assigned to a grafted *cis*-[Co(en)$_2$-
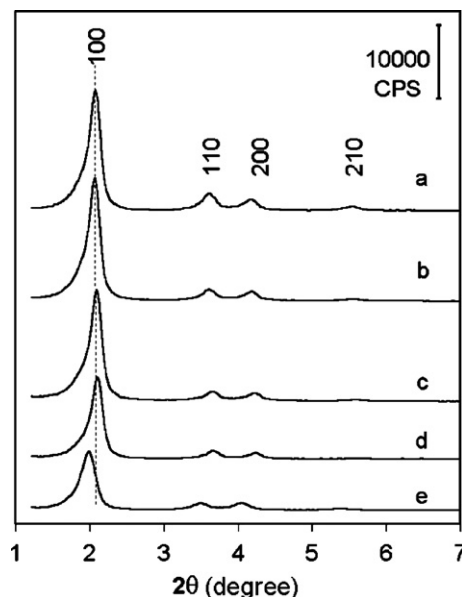

Fig. 2. XRD powder patterns of MTS: (a) acid washed, (b) silylated using HMDSA in toluene (method B) and acid washed, (c) silylated using HMDSA vapor (method C) and acid washed, (d) as in "b" and cation exchanged using a cobalt complex (see text) and (e) silylated using CTMS and HDMSO mixture (method A).

(OH)($\equiv$SiO)] cobalt complex according to an Extended X-ray Absorption Fine Structure (EXAFS) study [43]. Here, the adsorbed cobalt complex which is not removed by washing using ethanol is likely to be similar to that reported earlier [40,41,43] showing that the silylation using method B or C leaves some of the surface with silanol groups accessible to ion exchange and grafting.

The adsorption–desorption properties were measured on acid washed sample (Fig. 3). All the samples exhibit type IV isotherm typical of mesoporous materials [44]. The quite steep edge relative pressure p/p_0 of *ca.* 0.30 typical of narrow pore size distribution is preserved of the silylation. The height of the adsorption plateau, which is a measure of the pore volume, reveals a loss of internal volume of *ca.* 10%, 18% and 35% after silylation using method B, C and A, respectively (Fig. 3). There is also a decrease of surface (Table 1) and pore size (Fig. 4) along the same sequence as follows:

Not silylated > silylated in solution(method B)

$$> \text{silylated in gas phase(method C)}$$

$$> \text{silylated in solution using CTMS(method A)}$$

(1)

This order matches the silylation deepness calculated in terms of number of trimethylsilane (TRMS) functions per nm^2 obtained from elemental analysis of carbon performed on the acid washed solids according to following equation (Table 1) [38,45]:

$$S = \left[\frac{(\%C)}{50 - (\%C)} \right] \frac{N_A}{(\text{TRMS})(S_{\text{MTS}})} \times 10^{-18}$$
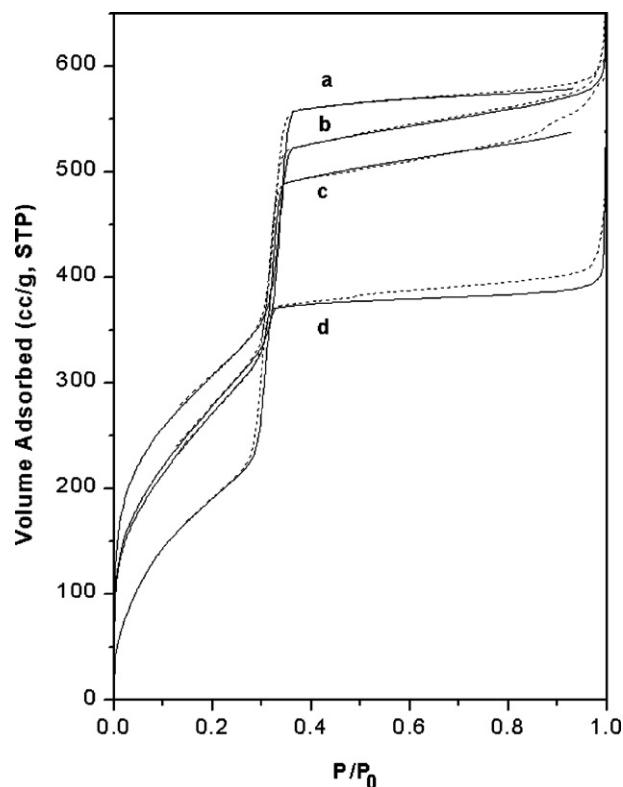
(2)

Fig. 3. Nitrogen adsorption–desorption curves of MTS: (a) acid washed, (b) silylated using a solution of HMDSA in toluene (method B), (c) silylated using HMDSA vapor (method C), above samples are acid washed and (d) silylated using CTMS and HMDSO (method A).
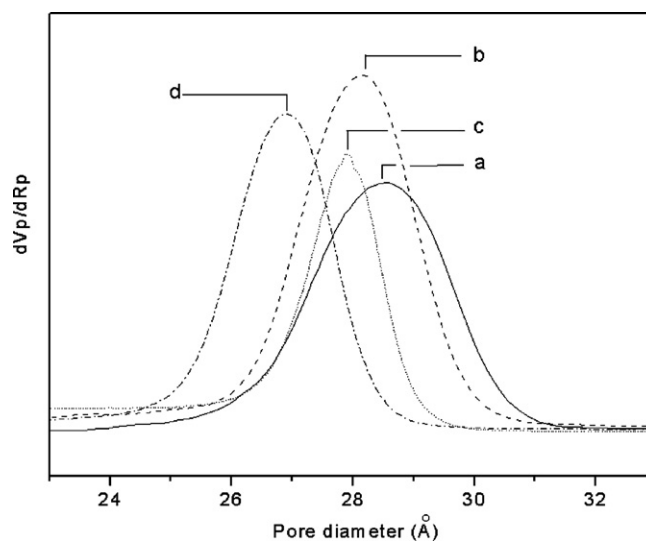

Fig. 4. BJH pore size distribution of MTS: (a) acid washed (—), (b) silylated using a solution of HMDSA in toluene (method B) and acid washed (---), (c) silylated using HMDSA vapor (method C) and acid washed (. . .), above samples are acid washed and (d) silylated using CTMS and HMDSO (method A) (-·-·-).

where %C is the content of carbon reported in weight percentage, N_A is Avogadro's number, TRMS is the effective molecular weight of trimethylsilyl (as

72 g/mol, considering the loss of one surface hydrogen per attached TRMS group) and S_{MTS} is the surface area of non-silylated material (1060 m^2/g in the present experiment). The concentrations of silanolate obtained by titration decreases also along the same sequence given above. All the data as well as those of the literature are reported in Table 1 in terms of number of CTMA$^+$ retained per nm^2 in the solid before or after silylation using the following equations:

Table 1
Textural properties of MTS and silylated materials

Entry	Sample[a]	d_{100} (Å)	SiO$^-$/ SiO$_2$ (%)	Surface area (m^2/g)	Pore diameter (BJH)/Å	N_{sur} (CTMA$^+$/ nm^2)	S (TRMS/ nm^2)	TRMS coverage (%)	Reference[b]
1	TMS-E	42.4	16.7	1060	28.5	1.6	0	0	tw
2	TMS-DM-B	42.1	13.8	919	28.0	1.3	1.1	42	tw
3	TMS-DM-C	42.0	9.4	883	27.9	0.9	1.6	61	tw
4	TMS-DM-A	44.6	0	655	26.9	0	2.6	100	tw
5	Large pore-C	–	–	915	56.5	–	–		[20]
6	Large pore-DM	–	–	540	52.5	–	1.8		[20]
7	MCM-41-C	–	–	1180	9.4	–	–		[50]
8	MCM-41-CM	–	–	925	25.3	–	0.6		[50]
9	MCM-41-E	–	–	1153	30.0	–	–		[50]
10	MCM-41-EM	–	–	829	24.0	–	0.7		[50]
11	FSM-16-C	–	–	1024	37.3	–	–		[51]
12	FSM-16-CM	–	–	734	32.7	–	1.5		[51]
13	S-157	–	–	750	–	–	2.0		[38]

(5, 6) Large pore MCM-41 direct silylated using CTMS and pyridine [18]. (7-10) Trimethylsilylation of MCM-41-C and MCM-41-E was done using CTMS in toluene [50]. (11, 12) FSM-16-C was modified as in c [51]. (13) Commercial silica (Fisher) silylated using HMDSA in toluene [38].
[a] MTS = Mesoporous templated silica, E = surfactant extracted using HCl ethanol solution, DM = directly trimethylsilylated, C = calcined, CM = calcined then trimethylsilylated, EM = surfactant extracted then trimethylsilylated.
[b] tw = This work, the numbers refer to the reference list.

$$\sigma(\equiv\text{SiO}^-) = \sigma(\text{CTMA}^+) \tag{3}$$

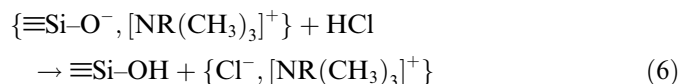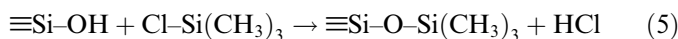$$N_{\text{sur}} = \frac{(\text{CTMA}^+/\text{SiO}_2\ \%)N_A}{60 \times (S_{\text{MTS}})} \times 10^{-20} \tag{4}$$

where $\sigma(\equiv\text{SiO}^-)$ and $\sigma(\text{CTMA}^+)$ are the number of SiO^- and CTMA^+ functions or ions per nm^2, $\text{CTMA}^+/\text{SiO}_2\ \%$ is the surfactant to silica mole percentage that is equal to the silanolate to silica mole percentage. The calculation reported in Table 1 shows that the number of CTMA^+ in the as-synthesized material is smaller than the number of silanol groups that can be silylated (1.6 in comparison to 2.6/nm^2). Furthermore, it appears that all three silylation methods used here displace more or less the surfactant. These points will be discussed below.

To facilitate the band assignment and the comparison between materials, the IR spectra have all been calibrated using the asymmetric bending vibrational mode of the SiO$_4$ units at 450 cm^{-1} (Fig. 5). The spectra have been divided in four regions to optimize the scale for the sake of clarity. The high frequency range (2600–4000 cm^{-1}) comprises the stretching vibrational mode of silanol groups ($v_{\text{O–H}}$) and, those of methylene and methyl groups ($v_{\text{C–H}}$) of the surfactant and TRMS groups. The next range 1300–1800 cm^{-1} contains the deformation vibrational mode $\delta_{\text{O–H}}$ of H$_2$O at approximately 1660 cm^{-1} (shifted at 1630 cm^{-1} in silylated samples) and $\delta_{\text{C–H}}$ of the alkyl chains between 1500 and 1350 cm^{-1}. In the range 900–1300 cm^{-1}, three strong bands at approximately 960, 1100 and 1250 cm^{-1} belong to the asymmetric stretching bends of the SiO$_4$ units [46–48]. At 800 cm^{-1} arises the forbidden symmetric stretching mode of SiO$_4$ units [47]. The $v_{\text{C–H}}$ and $\delta_{\text{C–H}}$ modes, which attest the presence of the surfactant in the as-synthesized and partially silylated materials, are absent in the material treated according to method

A. In the ranges 700–1300 cm^{-1} sharp features (marked by a star) appear for silylated samples only. The latter arising at 1260 cm^{-1}, 850 cm^{-1} (shoulder at 866 cm^{-1}) and 760 cm^{-1} are attributed to asymmetric stretching mode of the [SiOC$_3$] unit of the TRMS group. Their evolution is consistent with the silylation deepness mentioned above.

Another striking feature in the series of spectra is the absence of the peak at 960 cm^{-1} in the most silylated materials (method A, Fig. 5b–d). By contrast, the most intense peak in the this region arises at 970 cm^{-1} for the as-synthesized MTS. According to the literature on zeolite materials [47,49] this mode can be assigned to SiO$^-$ groups consistent with their high concentration in those types of samples. In addition, the evolution along this series of spectra suggests that the shoulder at 1090 cm^{-1} and the well defined peak at 1230 cm^{-1} can be also associated to the stretching modes of silanolate groups. Going back to the high frequency ranges, it appears clearly that the sample containing the largest amount of silanol groups (and water, see band at 960 cm^{-1}) is the as-synthesized MTS. Conversely, the fully silylated samples contains the smallest amount of water and still exhibits the fingerprints of associated silanol groups at *ca.* 3500 cm^{-1}.

The IR data are consistent with the literature according to the following equations [18]:

$$\equiv\text{Si–OH} + \text{Cl–Si(CH}_3)_3 \rightarrow \equiv\text{Si–O–Si(CH}_3)_3 + \text{HCl} \tag{5}$$

$$\{\equiv\text{Si–O}^-, [\text{NR(CH}_3)_3]^+\} + \text{HCl}$$
$$\rightarrow \equiv\text{Si–OH} + \{\text{Cl}^-, [\text{NR(CH}_3)_3]^+\} \tag{6}$$

Since an excess of reactant is used, all the accessible silanol groups are silylated and all CTMA$^+$ (SP groups) are removed using method A. By contrast, when the silylation is performed using HMDSA, NH$_3$ evolves instead of
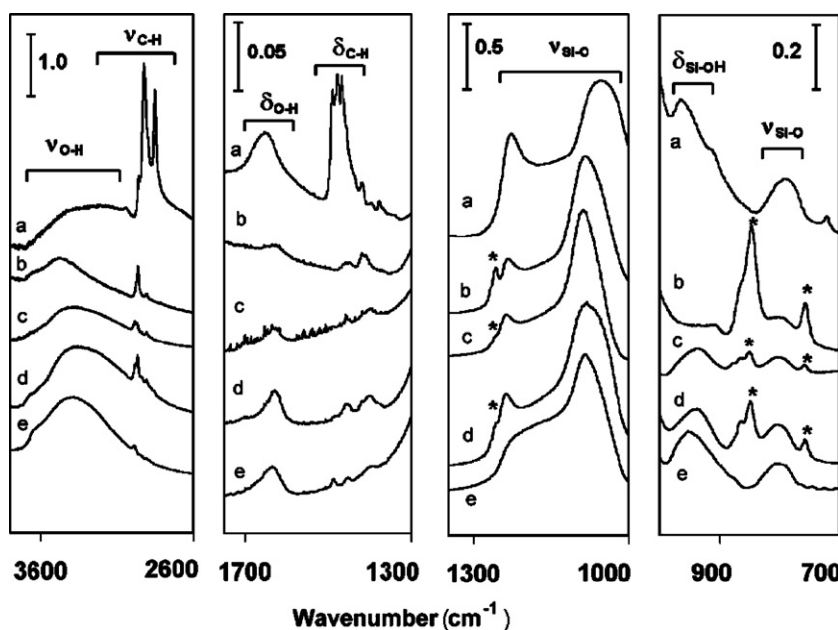

Fig. 5. FT-IR absorption of (a) as-synthesized MTS, (b) silylated-MTS according to method A and, in the following, the materials are acid washed to remove the surfactant, (c) silylated MTS using HMDSA in toluene (method B), (d) MTS silylated from gas phase HMDSA (method C), (e) MTS.

HCl. Contrary to the latter, the former cannot displace the surfactant (SP group). Therefore the only reaction that can take place is the following:

$$2\equiv Si–OH + NH[–Si(CH_3)_3]_2$$
$$\rightarrow 2\equiv Si–O–Si(CH_3)_3 + NH_3 \qquad (7)$$
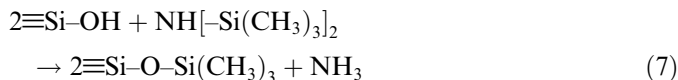
This is consistent with methods B and C yielding partial silylation, though a slight displacement of surfactant is still to be explained. Since the $CTMA^+$ cations have to be displaced together with an anion, the only mechanism available is the dissociation of water molecules yielding hydroxyl anions according to following equation:

$$\{\equiv Si–O^-, [NR(CH_3)_3]^+\} + H_2O \rightleftarrows \equiv Si–OH$$
$$+ \{OH^-, [NR(CH_3)_3]^+\} \qquad (8)$$
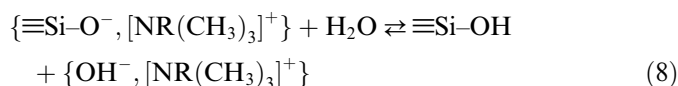
Such mechanism is expected to be favored when silylation is performed at higher temperatures for a long time or when CTMAOH is removed out of the catalysts bed. This is consistent with method C leading to a deeper silylation than method B.

In the following, nuclear magnetic resonance of ^{13}C nucleus is used to monitor the presence of the surfactant, to check the formation of surface trimethylsilyl groups and to further characterize the distribution of the groups on the surface (Fig. 4). The NMR resonances associated to CTMA arise at 14.5, 23.3, 30.5, 32.6, 54.2 ppm. They are respectively assigned to C16 (methyl end chain group), C2 and C15 (methylene groups at both extremity of the chain), C3 (third methylene group within the chain), C4–C13 (internal methylene groups), C14 and methyl groups of the ammonium head [52]. The broad peak at ca. 67 ppm is assigned to the first carbon C1 of the alkyl chain attached to the polarhead. The resonance near 0 ppm is assigned to the methyl group of the trimethylsilyl function [53]. Two other resonances arising at 16.3 and 58.4 ppm are observed on the solid treated using a HCl–ethanol solution. These peaks which disappear after treatment under vacuum at 150 °C (Figs. 4d and 5), are assigned to carbon bonds of the ethyl fragment of ethoxysilane groups (Si–OET) formed by esterification of the silanol groups [54,55].

The absence of resonance due to the surfactant in the sample treated according to method A (Fig. 6g) confirms their complete removal consistent with FT-IR data (vide supra). By contrast, samples treated according to methods B and C exhibit a strong signal of surfactant. The chemical shifts are unchanged except for C16, the signal of which is broader and less shifted after treatment using method C. This effect is more pronounced after treatment using method B. In addition, there are small signals appearing on the left or right side of the C16 signal. Though these changes are not yet fully understood, they indicate a change of conformation or a higher rate of motion at the end of the long alkyl chain of the quaternary ammonium. This is likely due to a different quality of packing of surfactants in partially silylated samples.
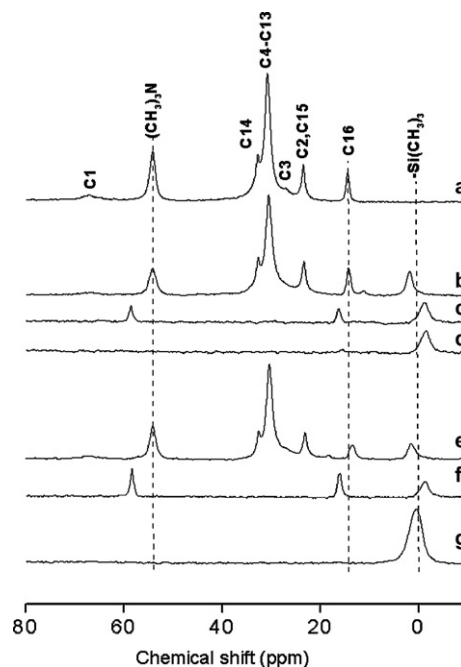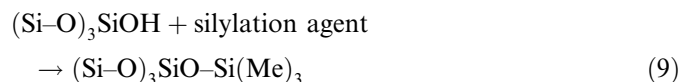

Fig. 6. ^{13}C-MAS-NMR spectra of (a) as-synthesized MTS (non-silylated); following materials are silylated-MTS using (b) HMDSA (method C), (c) as in "b" followed by acid washing, (d) as in "c" then heated at 150 °C, (e) HMDSA (method B), (f) as in "e" followed by acid washing, (g) CTMS (method A).

Nonetheless, the most sensitive feature is the chemical shift of the methyl groups held by the tethered trimethylsilyl moieties. For fully silylated samples (method A), the chemical shift (0.8 ppm) matches the value of the literature [56]. In comparison for partially silylated samples, ^{13}C resonance of the trimethylsilyl is deshielded (higher chemical shift of ca. 1.8 ppm) (Fig. 6b and e). By contrast, the sample treated using acid–ethanol solution exhibits a high shielded ^{13}C resonance of the TRMS groups (−0.7 ppm) before and after evacuation of ethanol at 150 °C. The ^{13}C resonance arises at the same place for fully silylated samples. This rather striking evolution affecting all the trimethylsilyl groups shows that, in partially silylated samples, there is sparse packing of such groups, which all are sensitive to changes in their close environment. This is further discussed below.

The same series were further investigated using ^{29}Si MAS NMR. All the samples exhibit two strong peaks at −108 and −98 ppm, and a shoulder at ca. −90 ppm assigned to Q_4, Q_3 and Q_2 species, respectively (Fig. 7) [57–59]. For silylated samples, there is one new feature (and even two in one of the cases) in the range of 5–20 ppm, assigned to the trimethylsilyl groups. The relative increase of Q_4 and $–Si(Me)_3$ species at the expense of Q_3 ones is quantitatively consistent with the silylation reaction [14,15]:

$$(Si–O)_3SiOH + silylation\ agent$$
$$\rightarrow (Si–O)_3SiO–Si(Me)_3 \qquad (9)$$

In addition, the chemical shift of both Q_3 and Q_4 species decreases from −98 to −102 and from −108 to
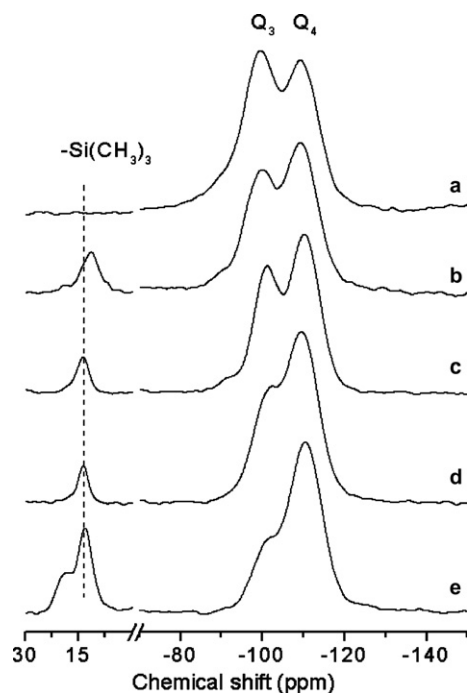
Fig. 7. ^{29}Si MAS-NMR spectra of (a) as-synthesized MTS (non-silylated), (b) silylated-MTS using HMDSA (method B), (c) same as "b" followed by acid washing, (d) same as "c" followed by evacuation at 150 °C under vacuum, (e) fully silylated sample using method A.

−112 ppm, respectively. Both fully silylated and partially silylated samples that were acid washed and evacuated exhibit the highest of chemical shift decreases, i.e. the highest shielding. An intermediate chemical shift of −100 ppm is measured for acid washed (but not evacuated) samples, the surface of which is partially esterified by the solvent ethanol leading to [Si(OSi)$_3$OEt] type of Q$_3$ species [58].

On the ^{29}Si spectra (like in ^{13}C spectra), this is also the signal assigned to the tethered TRMS groups that is the most affected by changes of molecular neighborhood. The highest shielding (11.5 ppm) occurs on ^{29}Si nuclei of partially silylated samples in presence of the surfactant (corresponding to the lower ^{13}C shielding of the methyl group). Conversely, the fully silylated sample shows the most deshielded ^{29}Si nuclei at 19.5 and at 13.5 ppm. Similar shifts than the latter are observed for signals of partially silylated samples when the surfactant is removed. Both signals at 13.5 and 19.5 ppm have been already reported in the literature without any comments [36,59,60].

4. Discussion

The data obtained from chemical analysis, FT-IR, ^{13}C and ^{29}Si solid state NMR are consistent with an increasing degree of trimethylsilylation moving from method B to C and, A, respectively. Along the same sequence, the decreasing intensity of the band at 1630 cm^{-1} attests the lesser wettability of the materials. In the following the surface species are first discussed in a qualitative manner from both NMR and IR data, then an overall picture of the modified surface is drawn, taking into account the surface coverage by TRMS groups.

The most striking points reside in the chemical shifts on ^{29}Si and ^{13}C spectra that are related to the electronic structure of the groups: the higher the electron density on a nucleus, the higher the shielding, resulting in an up-field shift (or a lower chemical shift). In addition, we shall take into account the eventual ring current due to electrically charged entities. It is also worth recalling that the up-field shift of the ^{29}Si resonance when oxygen replaces carbon around Si atom is due to a strong π_{d-p} character of the Si–O bond. The latter originates from donation of p electrons of non-banded pairs of oxygen into empty d orbitals of Si. Therefore, this shift depends on the hybridization of oxygen and on the substituent X held by oxygen in Si–O–X. A wider angle leads to a higher π back-donation and a higher up-field shift [57,61]. By contrast, a σ donor group, X, will weaken the Si–O bond and decrease the π effect yielding a downfield shift. This is consistent with the chemical shifts at 20.7, 17.7 and 14.6 ppm in the (Me)$_3$SiOEt, (Me)$_3$SiOMe and (Me)$_3$SiOH, respectively [62]. Accordingly, we will observe the following order of chemical shift for all the species:

$$\text{TRMS}_{SA} < \text{TRMS}_{LA} < Q^3\text{–OEt} < Q^3\text{–OMe} < Q^3\text{–OH}$$
$$< Q^3\text{–O}^- \leqslant Q^4_{SA} < Q^4_{LA}$$
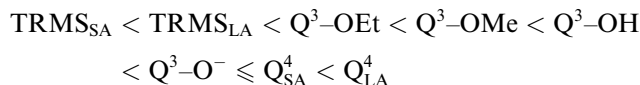
where the subscripts SA and LA stand for small and large Si–O–Si angles, respectively. The present spectra are consistent with this interpretation except for the Q^3–O$^-$ species that resonates at a smaller field than Q^3–OH and Q^3–OEt (see discussion below). In addition, one should observe a correlation between that shift on ^{29}Si and the shift of ^{13}C in the TRMS species. Indeed, when the ^{29}Si is shifted up-field consist with a stronger Si–O bond and a larger Si–O–Si angle, the Si–C bond of the TRMS moieties should be weaker (less σ donation from C to Si) yielding by compensation to an up-field shift of the ^{13}C resonance. Taking the chemical shift of ^{13}C as a probe, the Si–O–Si bridge angle should increase according to the following sequence (Fig. 8):

TRMS in presence of surfactant(Fig.8.3)

   < fully silylated sample(Fig.8.2)

   < partially silylated sample(Fig.8.1)

The same ranking should results from the ^{29}Si chemical shift. However, the partially silylated samples still containing the surfactant do not follow the expected correlation between the shifts of the ^{13}C and ^{29}Si spectra of the TRMS species. In addition, in these samples, the Q^3 resonance is shifted down field, which at odds with the expectation knowing that a large contribution is due to silanolate groups (see the ranking of Q^3–O$^-$ in the sequence provided above). These inconsistencies which cannot come from the electron distribution within the TRMS and the silanolate groups are likely due to positive charge of ammonium heads of surfactant.
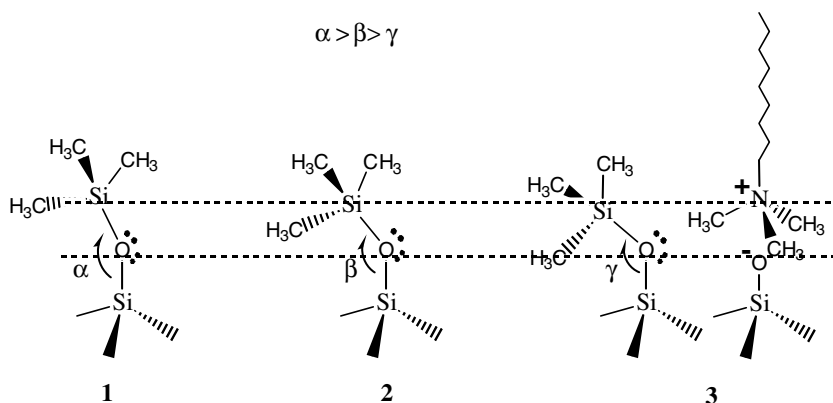
Fig. 8. Various types of TRMS groups on the surface.

According to this interpretation, most of the TRMS groups in partially silylated samples are nearby a hydrophilic region of the surface. Such distribution on the surface has been obtained most likely because the silylation has taken place between the head of the quaternary ammonium surfactant neutralizing the silanolate species (the latter are evenly distributed on the surface because of mutual electric repulsion). The TRMS group might be envisioned as stick fence posted in between the surfactant heads. When the surfactant is removed, the fingerprints of the ammonium heads remain as hydrophilic nanopatches.

Such a model implies some steric considerations and a surface coverage by both TRMS and surfactant head groups. The van der Waals radius of a trimethylammonium head of the surfactant is 0.334 nm leading to a surface occupancy of $0.35 \, \text{nm}^2$ [63]. In the as-synthesized form (Table 1, entry 1), the value of $1.6 \, \text{CTMA/nm}^2$ indicates that only 44% of surface is covered by trimethyl ammonium surfactant head groups (Table 1). Therefore, there is some room left for silylation that can be calculated using the van der Waals radius of TRMS. This is 0.37 nm leading to a surface occupancy of $0.43 \, \text{nm}^2$ per group [38]. Therefore the number of TRMS groups that should fit in between the surfactant head groups is $1.02/\text{nm}^2$. Silylation according to method B (Table 1, entry 2), leads to a TRMS density slightly higher than this feature ($1.1 \, \text{TRMS/nm}^2$) consistent with a slight displacement of the surfactant the coverage of which drops down (from 1.6 to $1.3 \, \text{CTMA/nm}^2$) and an overall surface coverage of 93%. The deeper silylating route, method C (Table 1, entry 3) displaces further the surfactant and yields a surface coverage of 100%. Strikingly, method A, which displaces all the surfactant yields a TRMS density of $2.6/\text{nm}^2$, higher than theoretical limit of $2.33 \, \text{TRMS/nm}^2$. Most of the TRMS surface densities reported in the literature indeed fall below this the theoretical limit (Table 1, and Ref. [64]). However, TRMS packing as high as 2.45 and $2.7/\text{nm}^2$ were also reported for amorphous silica using HMDSA [65] and CTMS [66] as silylation agent, respectively. Though quite high, these values were not discussed in the previous reports. This overpacking is probably due to the fact that TRMS groups are tilted, thus decreasing their projected area and/or to the fact that the surface is not flat.

5. Conclusion

The effect of the various methods of silylation on the surface coverage and on the properties of hexagonal micelle templated silicas was studied using BET surface measurement, pore size distribution, FT-IR and ^{13}C and ^{29}Si MAS NMR. Direct silylation of micelle templated silica still containing the templating surfactant can lead to total or partial silylation of the internal (and external) surface depending on the silylation agent. A mixture of chlorotrimethylsilane in hexamethyldisiloxane leads to full coverage by trimethylsilyl groups and to a very hydrophobic surface. Using hexamethyldisilazane, the silylation drops down to 45–65% and displaces only partially the templating $CTMA^+$ surfactant. The displacement of the remaining surfactant molecules leaves behind hydrophilic nests of the size of the ammonium heads ($\sim 0.7 \, \text{nm}^2$). Cation exchange can be performed on these nests at pH to 10 without structure collapse.

References

[1] C.T. Kresge, M.E. Leonowicz, W.J. Roth, J.C. Vartuli, J.S. Beck, Nature 359 (1992) 710.
[2] D. Brunel, Micropor. Mesopor. Mater. 27 (1999) 329.
[3] J.H. Clark, D.J. Macquarrie, Chem. Commun. (1998) 853.
[4] M.R. Ganjali, L. Hajiagha Babaei, A. Badiei, K. Saberian, S. Behbahani, G. Mohammadi Ziarani, M. Salavati-Niasari, Quim. Nova. 29 (2006) 440.
[5] D.C. Sherrington, A.P. Kybett, in: Proceedings of the 4th International Symposium on Supported Reagents and Catalysis in Chemistry, Supported Catalysts and their Applications, RSC Pubs., UK, 2001.
[6] L. Bonneviot, F. Béland, C. Danumah, S. Giasson, S. Kaliaguine, in: Proceedings of the 1st International Symposium on Mesoporous Molecular Sieves Stud. Surf. Sci. Catal., vol. 117, Elsevier, Amsterdam, Baltimore, 1998.
[7] J.M. Kim, R. Ryoo, Bull. Korean Chem. Soc. 17 (1996) 66.
[8] R. Ryoo, S. Jun, J. Phys. Chem. B 101 (1997) 317.
[9] M.V. Landau, S.P. Varkey, M. Herskowitz, O. Regev, S. Pevzner, T. Sen, Z. Luz, Micropor. Mesopor. Mater. 33 (1999) 149.

[10] D. Zhao, J. Feng, Q. Huo, N. Melosh, G.H. Fredrickson, B.F. Chmelka, G.D. Stucky, Science 279 (1998) 548.
[11] N. Coustel, F. DiRenzo, F. Fajula, J. Chem. Soc., Chem. Commun. (1994) 967.
[12] R. Mokaya, J. Phys. Chem. B 103 (1998) 10204.
[13] K.A. Koyano, T. Tatsumi, Y. Tanaka, S. Nakata, J. Phys. Chem. B 101 (1997) 9436.
[14] X.S. Zhao, G.Q. Lu, J. Phys. Chem. B 102 (1998) 1556.
[15] N. Igarashi, Y. Tanaka, S. Nakata, T. Tatsumi, Chem. Lett. (1999) 1.
[16] M. Park, S. Komarneni, Micropor. Mesopor. Mater. 25 (1998) 75.
[17] S. Abry, B. Albela, L. Bonneviot, C.R. Chimie 8 (2005) 741.
[18] V. Antochshuk, M. Jaroniec, Chem. Commun. (1999) 2373.
[19] D. Das, C. Tsai, S. Cheng, Chem. Commun. (1999) 473.
[20] R. Ryoo, S. Jun, J. Phys. Chem. B 101 (1997) 317.
[21] J.M. Kim, S. Jun, R. Ryoo, J. Phys. Chem. B 103 (1999) 6200.
[22] C. Yoshina-Ishii, T. Asefa, N. Coombs, M.J. MacLachlan, G.A. Ozin, Chem. Commun. (1999) 2539.
[23] S. Inagaki, S. Guan, T. Ohsuna, O. Terasaki, Nature 416 (2002) 304.
[24] P. Sutra, D. Brunel, Chem. Commun. (1996) 2485.
[25] X. Feng, G.E. Fryxell, L.-Q. Wang, A.Y. Kim, J. Liu, K.M. Kemner, Science 276 (1997) 923.
[26] D.S. Shephard, W. Zhou, T. Maschmeyer, J.M. Matters, C.F.G. Johnson, M.J. Duer, Angew. Chem., Int. Ed. 37 (1998) 2719.
[27] W.M. Van Rhijn, D.E. De Vos, B.F. Sels, W.D. Bossaert, P.A. Jacobs, Chem. Commun. (1998) 317.
[28] M.H. Lim, A. Stein, Chem. Mater. 11 (1999) 3285.
[29] K. Moller, T. Bein, R.X. Fischer, Chem. Mater. 11 (1999) 665.
[30] M.H. Lim, C.F. Blanford, A. Stein, Chem. Mater. 10 (1998) 467.
[31] T. Tatsumi, J. Porous Mater. 6 (1999) 13.
[32] T. Tatsumi, K.A. Koyano, N. Igarashi, Chem. Commun. (1998) 325.
[33] X.S. Zhao, G.Q. Lu, X. Hu, Chem. Commun. (1999) 1391.
[34] K.M. Reddy, C. Song, Catal. Lett. 36 (1996) 103.
[35] L. Chen, T. Horiuchi, T. Mori, K. Maeda, J. Phys. Chem. B 103 (1999) 1216.
[36] T. Yanagisawa, T. Shimizu, K. Kuroda, C. Kato, Bull. Chem. Soc. Jpn. 63 (1990) 1535.
[37] C.W. Lentz, Inorg. Chem. 3 (1964) 574.
[38] D.W. Sindorf, G.E. Maciel, J. Phys. Chem. 86 (1982) 5208.
[39] A.-R. Badiei, S. Cantournet, M. Morin, L. Bonneviot, Langmuir 14 (1998) 7087.
[40] A.-R. Badiei, L. Bonneviot, Inorg. Chem. 37 (1998) 4142.
[41] R.L. Burwell, R.G. Pearson, G.L. Haller, P.B. Tjok, P.S. Chock, Inorg. Chem. 4 (1965) 1123.
[42] G. Engelhardt, U. Lohse, A. Samoson, M. Magi, M. Tarmak, E. Lippmaa, Zeolites 2 (1982) 59.
[43] F. Béland, A.-R. Badiei, M. Rönning, D. Nicholson, L. Bonneviot, Phys. Chem. Chem. Phys. 1 (1999) 605.
[44] K.S.W. Sing, D.H. Evertt, R.A.W. Haul, L. Moscou, r.A. Pierotti, J. Rouquerol, T. Siemieniewska, Pure Appl. Chem. 57 (1985) 603.
[45] S.M. Holmes, V.L. Zholobenko, A. Thursfield, R.J. Plaisted, C.S. Cundy, J. Dwyer, J. Chem. Soc. Faraday Trans. 94 (1998) 2025.
[46] A. Burneau, J.-P. Gallas, in: A.P. Legrand (Ed.), The Surface Properties of Silica, John Wiley & Sons, 1998, Chapter 3A.
[47] Y. Huang, Z. Jiang, W. Schwieger, Chem. Mater. 11 (1999) 1210.
[48] K. Nakamoto, Infrared and Raman Spectra of Inorganic and Coordination Compounds, Part: A, 5th ed., John Wiley, New York, 1997.
[49] R. Szostak, Molecular Sieves: Principles of Synthesis and Identification, Van Nostrand Reihold, New York, 1989, pp. 323–326.
[50] X.S. Zhao, G.Q. Lu, A.K. Whittaker, G.J. Millar, H.Y. Zhu, J. Phys. Chem. B 101 (1997) 6525.
[51] V. Antochshuk, M. Jaroniec, J. Phys. Chem. B 103 (1999) 6252.
[52] M. Fröba, P. Behrens, J. Wong, G. Engelhardt, C.H. Haggenmüller, G. Van De Goor, M. Rowen, T. Tanaka, W. Schwieger, Mater. Res. Soc. Symp. Proc. 371 (1995) 99.
[53] D.W. Sindorf, G.E. Maciel, J. Am. Chem. Soc. 105 (1983) 3767.
[54] G.S. Caravajal, D.E. Leyden, G.R. Quintingand, G.E. Maciel, Anal. Chem. 60 (1988) 1776.
[55] T. Kimura, K. Kuroda, Y. Sugahara, J. Porous Mater 2 (1998) 127.
[56] G.R. Hays, A.D.H. Clague, R. Huis, G. Van der Velden, Appl. Surf. Sci. 10 (1982) 247.
[57] G. Engelhardt, D. Michel, High-Resolution Solid-State NMR of Silicates and Zeolites, Wiley, New York, 1987.
[58] I-S. Chuang, G.E. Maciel, J. Phys. Chem. B 101 (1997) 3052.
[59] S. Haukka, A. Root, J. Phys. Chem. 98 (1994) 1695.
[60] K. Endo, Y. Sugahara, K. Kuroda, Bull. Chem. Soc. Jpn. 67 (1994) 3352.
[61] E. Duprez, R.F. Pettifer, Nature 308 (1984) 523.
[62] T.M. Alam, M. Henry, Phys. Chem. Chem. Phys. 2 (2000) 23.
[63] Calculation performed using Cerius2 molecular modelling (version 3.5) C–N–C angles of 109°54′, N–C bond distances of 0.148 nm, C–H bond distances of 0.110 nm, and hydrogen van der Waals radius of 0.120 nm.
[64] W.K. Lowen, E.C. Broge, J. Phys. Chem. 65 (1966) 16.
[65] A.C. Zettlemoyer, H.H. Hsing, J. Colloid Interface Sci. 58 (1977) 263.
[66] K.K. Unger, N. Becker, P. Paumeliotis, J. Chromatogr. 125 (1976) 115.